

## BASTITE PSEUDOMORPHS AFTER ORTHOPYROXENE, CLINOPYROXENE AND TREMOLITE

MICHAEL A. DUNGAN

Department of Geological Sciences, Southern Methodist University, Dallas, Texas 75275, U.S.A.

### ABSTRACT

Intergrowths consisting almost exclusively of lizardite platelets with bastite texture are pseudomorphic after orthopyroxene, clinopyroxene and tremolite, from which they are derived by topotactic reaction. Some bastites have inherited the high Al content of the original pyroxene, which may account for the predominance of lizardite in pyroxene bastites. Serpentine-dehydration reactions during progressive metamorphism of serpentinites explain why antigorite is the stable serpentine form in the presence of tremolite, forsterite and diopside. The low-temperature replacement of these phases by lizardite is in contradiction with some of the observed reactions. Phase relations in aluminous systems remain controversial. Secondary diopside is sporadically associated with bastites after both tremolite and clinopyroxene. Textural relations suggest that this diopside nucleated during the formation of associated bastites. The assemblage lizardite + diopside as a product of serpentinization may represent a metastable analogue of the assemblage diopside + antigorite.

### SOMMAIRE

Des intercroissances consistant presque exclusivement de plaquettes de lizardite à texture de bastite sont pseudomorphes de l'orthopyroxène, du clinopyroxène et de la trémolite, dont elles proviennent par réaction topotactique. Certaines bastites ont hérité leur haute teneur d'aluminium du pyroxène originel, ce qui expliquerait la prédominance de la lizardite dans ces bastites. Les réactions de déshydratation de la serpentine pendant le métamorphisme progressif des serpentinites rendent compte du fait que l'antigorite soit la forme stable en présence de trémolite, forstérite et diopside. Le remplacement à basse température de ces phases par la lizardite serait incompatible avec certaines des réactions observées: les relations de phases dans les systèmes alumineux restent sujettes à controverse. Le diopside secondaire associé aux bastites qui remplacent trémolite et clinopyroxène serait, d'après les relations texturales, contemporain des bastites. Les assemblages à lizardite et diopside, en tant que produits de serpentinisation, marquent peut-être l'analogue métastable de l'association antigorite + diopside.

(Traduit par la Rédaction)

### INTRODUCTION

This paper presents petrographic descriptions

of bastites after orthopyroxene, clinopyroxene and tremolite, and new data on the occurrence of secondary diopside formed in association with the serpentinization of clinopyroxene and tremolite. The purpose of this paper is to combine these petrographic observations and derive some constraints on the reactions involved in bastite formation. Microprobe analyses of various serpentine minerals and pseudomorphs, including bastites, are presented in a companion paper (Dungan 1979).

Investigations of serpentine petrology reported here and in accompanying papers (Dungan 1977, 1979) are an outgrowth of a broader structural and petrological project concerning ultramafic and mafic rocks in the Sultan area, North Cascades, Washington (Johnson *et al.* 1977, Vance & Dungan 1977, Vance *et al.* 1980). However, the mineralogical portion of the original project on serpentines was expanded to include samples of ultramafic rock from several additional localities. These localities are the Darrington (Vance 1972) and Weden Creek (Heath 1972) peridotites, which crop out in a belt adjacent to the Sultan bodies and the Feather River peridotite, northern Sierran foothills, California (Hietanen 1951, 1973, Ehrenberg 1975). Figure 1 is a generalized geological map of the Darrington-Sultan-Weden Creek area. The metamorphic history of the Darrington-Sultan peridotites and metaserpentinites is discussed in detail in Vance & Dungan (1977).

### PREVIOUS WORK ON BASTITES

Haidinger (1845) defined the term *bastite* as a serpentine pseudomorph after orthopyroxene, and its usage is similarly restricted in the *Glossary of Geology* (Gary *et al.* 1972). However, bastite also has been used to describe pseudomorphs after clinopyroxene and amphibole (Winchell & Winchell 1951, Klinkhammer 1962, Hochstetter 1965). I concur with Wicks & Whittaker (1977), who proposed that the term *bastite* be expanded to include a prefix indicating the identity of the parent mineral,

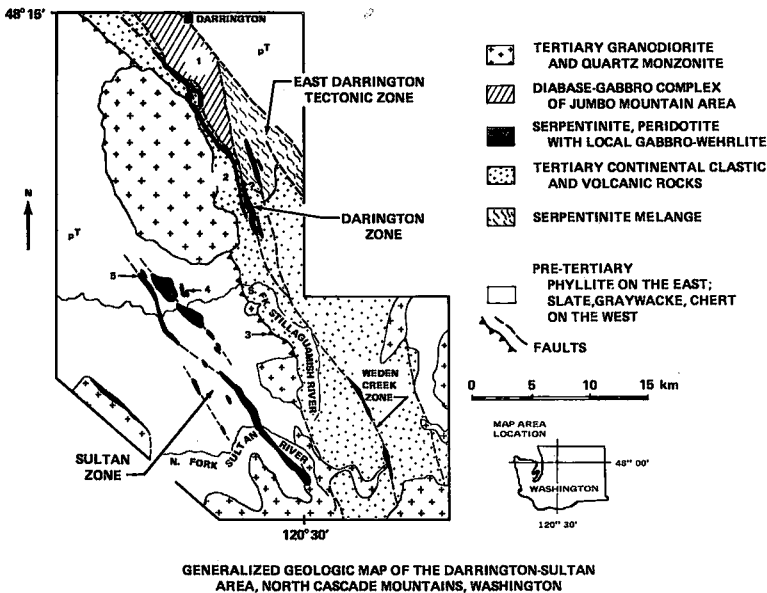


FIG. 1. Generalized geological map of the Darrington-Sultan area, Washington. Ultramafic rocks occur in two *en échelon* belts emplaced along high-angle faults and locally are intruded by Tertiary plutons.

*i.e.*, opx-bastite, cpx-bastite and amphibole-bastite or tremolite-bastite. Lizardite, the predominant mineralogical constituent of bastites, is characterized by variable orientations between its optic and crystallographic axes, resulting in occurrences of both length-fast and length-slow varieties (Wicks 1969, Wicks & Zussman 1975). Serpentine fibres with positive and negative elongation have been referred to as  $\gamma$ - and  $\alpha$ -serpentine, respectively. Although Wicks & Zussman (1975) have demonstrated that these distinctions do not necessarily have mineralogical significance, they have been adopted as petrographic terms (Francis 1956, Coats 1968, Wicks 1969) and are used in this paper in a strictly descriptive sense.

Recent studies by Wicks (1969), Wicks & Whittaker (1975, 1977) and Wicks & Zussman (1975) presented the most complete and detailed data concerning the mineralogy of serpentine textures. This paper draws heavily on the results of these studies, particularly the evidence that retrograde bastites are comprised dominantly of lizardite and that submicroscopic lizardite platelets in bastites are oriented with respect to the parent phases. Petrographic descriptions of bastites in Wicks & Whittaker (1977) are in essential agreement with observations made in this study. Wicks & Whittaker (1977) also included a complete list of references on bastite petrography and mineralogy. These will not be repeated here, since the more

recent studies by Wicks and others either incorporate or supersede the earlier works.

#### PETROGRAPHY OF THE BASTITES

##### *Opx-bastites*

Those Sultan serpentinites that have not been deformed or affected by the pre-emplacment or contact metamorphic events exhibit well-preserved cumulus textures, with orthopyroxene occurring as an intercumulus and cumulus phase. The serpentine pseudomorphs that replace orthopyroxene in the Darrington and Sultan peridotites are similar to opx-bastites described from many localities. The dominant feature of the internal structure of opx-bastites is the uniform replacement of the parent pyroxene by  $\gamma$ -serpentine, which parallels the [110] pyroxene cleavage (Figs. 2b, c). Typically, opx-bastites appear as smooth, featureless "plates" of  $\gamma$ -serpentine of uniform birefringence and extinction. Wicks & Zussman (1975) reported that the submicroscopic lizardite platelets that comprise opx-bastites exhibit only minor variations in orientation. Most opx-bastites are free of included magnetite and are colorless in plane-polarized light (Figs. 2b, c). Secondary serpentine that has replaced "primary" opx-bastite is present in some ultramafic rocks in the Sultan and Darrington areas. Bastites in some rocks that have been thermally upgraded are partly to completely replaced by antigorite or talc + chlorite.

### *Cpx-bastites*

The layered ultramafic cumulates in the Sultan area are generally clinopyroxene-rich. The most abundant rock-types are wehrlite and clinopyroxene-rich lherzolites, but all gradations to olivine-poor cumulates, including websterites, are present. Clinopyroxene typically occurs as a cumulus phase modified by adcumulus growth, resulting in large, branching clinopyroxene crystals (up to 1 cm) that partly or completely enclose smaller olivine grains in a subpoikilitic texture.

The majority of the cumulus ultramafic rocks in the northern Sultan area contain clinopyroxene that is unaltered except for the incipient development of diallage and the attendant formation of clear diopside overgrowths (Fig. 3). However, extensive sampling has revealed several examples of partial and complete serpentine pseudomorphs after clinopyroxene. The partial pseudomorphs (Figs. 2a, d) were extremely useful in establishing textural criteria for the recognition of cpx-bastites in completely serpentized rocks.

Except in a few localities, ultramafic cumulates in the southern Sultan area are completely serpentized. Based on textures in partly replaced clinopyroxenes, the presence of abundant clinopyroxene in the parent rocks is inferred.

As noted by Wicks & Whittaker (1977), cpx-bastites (Figs. 2d, e) do not develop into the relatively featureless plates of  $\gamma$ -serpentine that are characteristic of opx-bastites (Figs. 2b, c). Rather, the cpx-bastites almost invariably consist of low-birefringence intergrowths of  $\gamma$ - and  $\alpha$ -serpentine (lizardite). These intergrowths may be isotropic, but more commonly they consist of fine-grained serpentine intergrowths with a preferred orientation parallel to the cleavage of the parent clinopyroxene (Figs. 2c, d, e, f).

Additional differences between opx- and cpx-bastites are present in the Sultan serpentinites. Magnetite occurs with many cpx-bastites, both as rectangular networks intergrown with the lizardite and as rims surrounding partly serpentized clinopyroxenes (Fig. 2a). Although magnetite is present in some opx-bastites as disseminated blebs (Fig. 2c) or linear segregations, it rarely develops the extensive network characteristic of cpx-bastites. Finally, when viewed in plane light the cpx-bastites typically exhibit a pale-green or yellowish-green color in contrast to the colorless opx-bastites. Taken together, the textural criteria discussed above serve to distinguish cpx- and opx-bastites where they occur in the same thin section. However,

both types of pseudomorph encompass some textural variability; for example, in a significant number of samples in which both opx-bastites and cpx-bastites occur, magnetite is not extensively intergrown with the cpx-bastites and may even be more abundant in the opx-bastites. Some of the variability may be the result of the prograde effects documented by Wicks & Plant (1979).

### *Tremolite-bastites*

Tremolite occurs in two textural habits in olivine-rich metaserpentinites. The typical texture in statically recrystallized rocks, such as the Weden Creek peridotite, consists of radiating sheaves of tremolite needles piercing granular, subequant olivine or olivine + talc or olivine + antigorite. A second mode of occurrence is characterized by euhedral to subhedral tremolite grains, ranging in shape from stubby to highly elongate (length:width > 10:1) in a matrix of olivine. These amphiboles define a mineral lineation in several of the Feather River samples, suggesting that this second habit is favored by syntectonic recrystallization. Serpentinization of tremolite in the Weden Creek and the Feather River peridotites is widespread; it is interpreted as entirely retrograde in origin.

Contact-metamorphosed ultramafic rocks in the southern Sultan Complex are generally characterized by the assemblage forsterite + talc + tremolite. Serpentinization of this assemblage is advanced in some areas. The tremolite in these rocks is typically fine-grained, but two excellent examples of coarse-grained (> 5 mm), partly and completely serpentized tremolite were found (Fig. 4b).

Amphibole-bastites are readily distinguished from pyroxene-bastites on the basis of the distinctive habit of the parent amphibole. However, this criterion will not distinguish bastites after tremolite from those after anthophyllite. Two textural varieties of serpentine are present in tremolite-bastites, and their sequence of formation and relative abundances depend on several factors, including: (1) the prominence of the (001) parting in the amphibole, (2) the habit of the amphibole and (3) the degree of serpentinization of the matrix olivine. The serpentinization of tremolite is usually initiated by a pseudomorphic replacement of the amphibole parallel to its cleavage and along grain boundaries (Fig. 4a). The growth of  $\gamma$ -serpentine (usually lizardite) along the amphibole cleavage planes results in bastite textures that tend to resemble opx-bastites rather than cpx-bastites (Figs. 4b-h). The stage of initial replacement

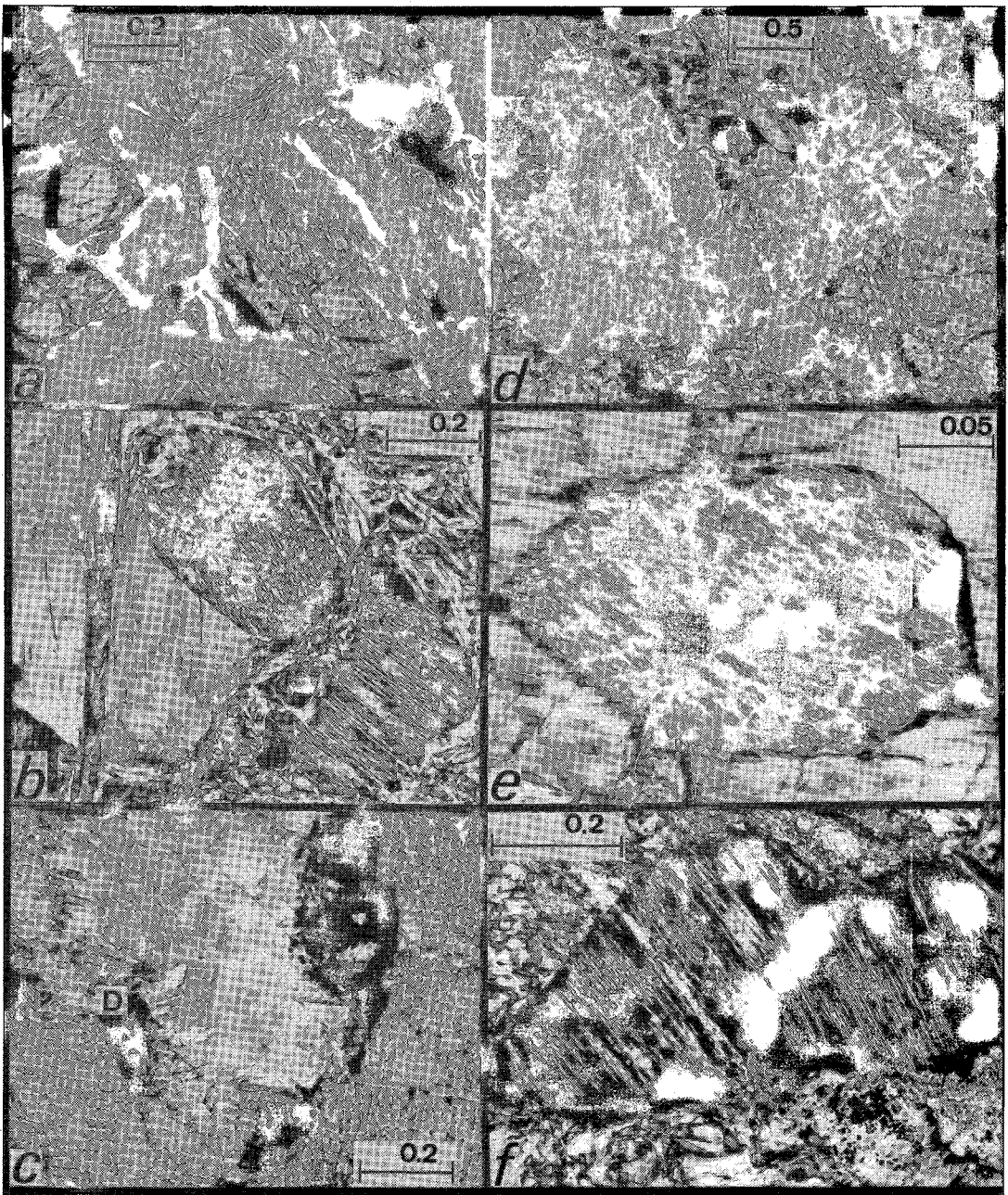


FIG. 2. (a) Sample 04-124, northern Sultan Complex. Clinopyroxene partly serpentinized to lizardite as  $\gamma$ -serpentine along cleavage planes. Note the abundance of magnetite associated with the cpx-bastites. Partly crossed polars. Scale in mm (as in b to f). (b) Sample 71-109, southern Sultan Complex. Opx-bastite (on left) is composed of a nearly featureless plate of  $\gamma$ -serpentine. Two cpx-bastites exhibit typical intergrowth of relatively high-birefringence  $\gamma$ -serpentine with isotropic serpentine. Bastites are set in a matrix of mesh-textured lizardite. Opx-bastite is cut by a shear zone of secondary serpentine. Magnetite associated with either type of pseudomorph is nearly lacking in this area. Crossed polars. (c) Sample 71-279, serpentinized clinopyroxene-rich websterite, southern Sultan Complex;  $\gamma$ -serpentine opx-bastite in the centre of the picture is surrounded by cpx-bastites. Magnetite is more abundant in opx-bastites than cpx-bastites in this sample. Post-serpentinization deformation has caused a set of slip surfaces to develop in opx-bastite normal to  $\gamma$ -serpentine fibre-direction. Elongate prisms of diopside (D) jut into the opx-bastite from margins of several cpx-bastites. Partly crossed polars. (d) Sample 71-268. Large subpoikilitic cpx-bastites include abundant magnetite as blades parallel to relict clinopyroxene cleavage

is usually advanced before the surrounding olivine grains exhibit more than incipient serpentinization. The degree of serpentinization of tremolite grains within a single thin-section varies, although in rocks in which the olivine is totally serpentinized, tremolite is also generally completely replaced. Where the (001) parting in the parent amphibole is particularly well developed, replacement along the parting occurs in the form of cross-veins consisting of  $\gamma$ - or  $\alpha$ -serpentine. Tremolite that occurs as sheaves of elongate needles rarely develops a good parting and, therefore, is rarely cut by cross-veins.

The growth of cross-veins in tremolite-bastites seems to be partly a function of the degree of serpentinization of the matrix olivine. The initial stages in the serpentinization of olivine are almost invariably represented by the growth of cross-fibre veinlets along the orthogonal parting of the olivine. In rocks that contain relatively coarse-grained olivine and large tremolite euhedra (e.g., Feather River peridotites), the early vein-forming stage in olivine is reflected in the amphibole-bastites by the growth of  $\alpha$ -serpentine (or very rarely,  $\gamma$ -serpentine) veinlets normal to the amphibole cleavage. These cross-fibre veinlets have a fibre direction normal to the long dimension of the vein. The cross-veins in the tremolite-bastites are commonly extensions of serpentine veinlets in the adjacent olivines. Where the veinlets are well developed and closely spaced a pseudomesh texture tends to form. This consists of orthogonal areas of  $\gamma$ -serpentine bastite, with or without a central core of unreplaced tremolite, whose boundaries are defined by the  $\alpha$ -serpentine veins (Figs. 4d, e). Despite the superficial resemblance of the cross-veined tremolite-bastites to the classic olivine mesh-texture, the timing of formation of the veins relative to the intervening "mesh centres" may not be as rigidly prescribed in tremolite-bastites. Whereas cross-veins may be early and may directly replace tremolite, the mode of vein formation may also be secondary in that some veins seem to replace earlier formed  $\gamma$ -serpentine rather than the parent mineral. The replacement of tremolite-bastites by "secondary" serpentine is further illustrated by the occurrence of irregular-shaped patches of  $\alpha$ -serpentine after  $\gamma$ -serpentine. These patches and veins are more abundant in com-

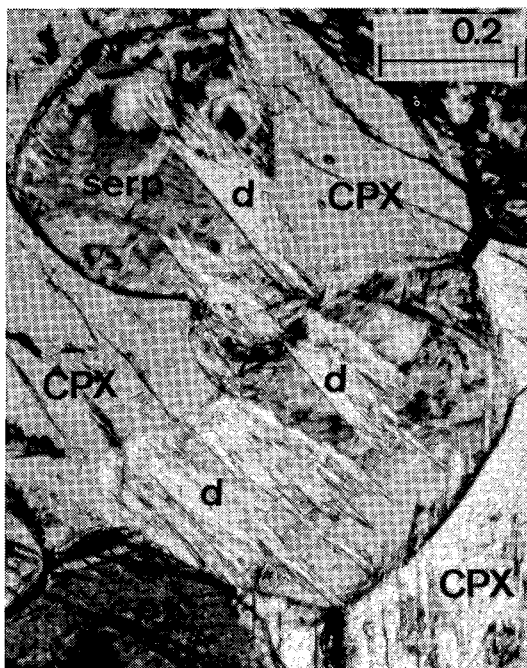


FIG. 3. Secondary bladed diopside (d) rims on primary clinopyroxene (cpx). Note that elongate diopside cross-cuts adjacent opx-bastites.

pletely serpentinized rocks.

An additional textural variety of serpentine sporadically associated with tremolite-bastites is a rim of  $\gamma$ -serpentine that occurs as radiating bundles oriented roughly normal to the grain boundaries of the bastite (Figs. 4e, f). The timing of formation of these rims is unclear, as is their textural significance.

#### SECONDARY DIOPSIDE

Peters (1968) recognized that diopside formed during the metamorphism of serpentinites is compositionally distinct from relict, primary clinopyroxenes in alpine peridotites. Evans & Trommsdorff (1970) subsequently demonstrated that diopside + antigorite is a stable assemblage in greenschist-facies metaserpentinites. Secondary diopside occurs as rims surrounding diallagic clinopyroxene (Fig. 3) and in association with pyroxene-bastites as rims and discrete grains. Secondary diopside has been identified positively or tentatively in several of the rocks containing tremolite-bastite from both the Feather River and the Sultan-Darrington areas.

planes. Matrix mesh-textured lizardite has recrystallized to antigorite. Partly crossed polars. (e) Sample 71-125. A small poikilitically enclosed clinopyroxene and the surrounding orthopyroxene are both pseudomorphed with typically contrasting results. The high-birefringent opx-bastite (magnetite-free) contrasts with the low-birefringent intergrowth (magnetite is present) characteristic of cpx-bastites. Crossed polars. (f) Sample 71-268. Typical cpx-bastites composed of high-birefringence lizardite as  $\gamma$ -serpentine in a matrix of low-birefringence to isotropic lizardite. Crossed polars.

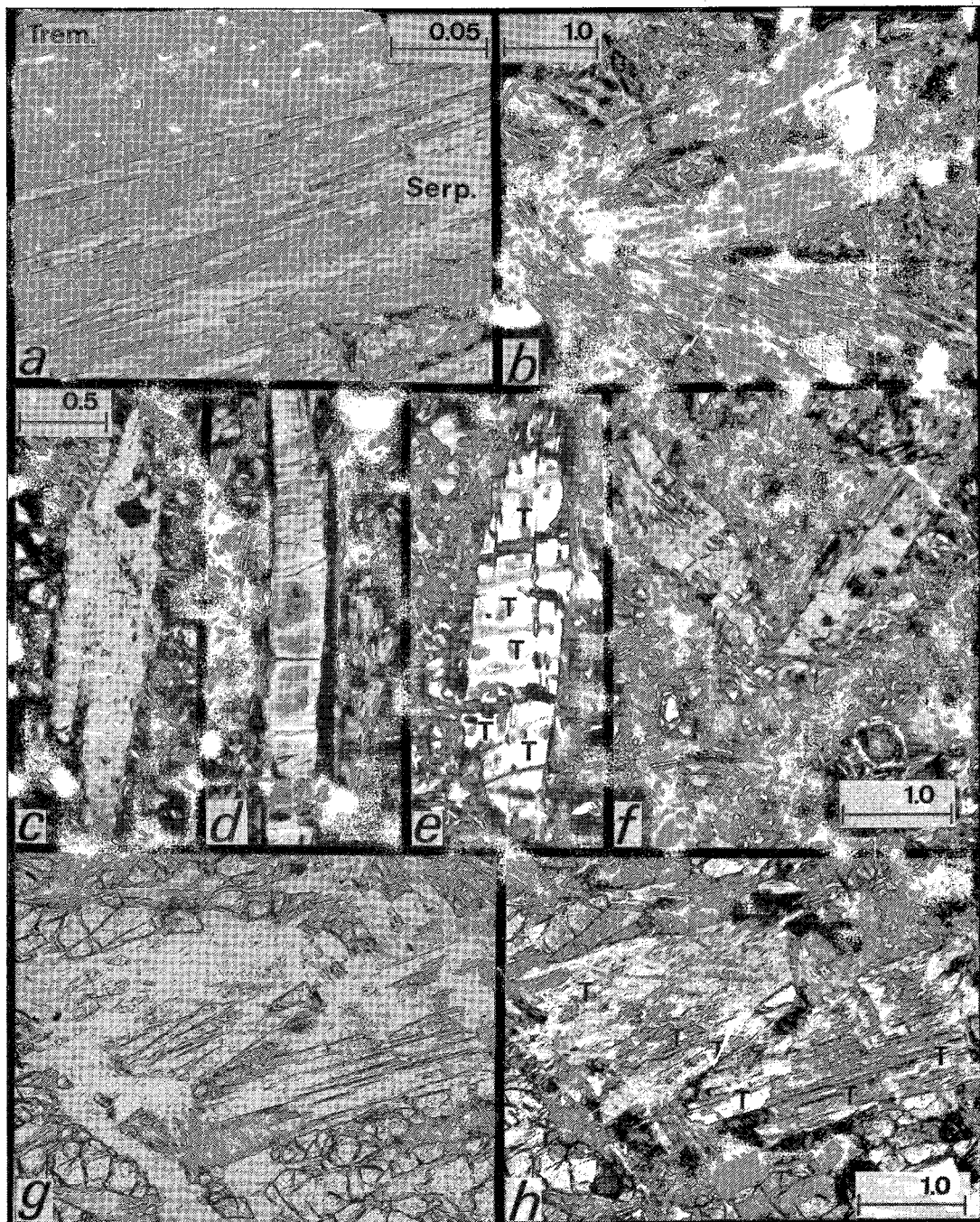


FIG. 4. Photomicrographs of tremolite-bastite: (a) Sample WC #4. Incipient replacement of tremolite (dark) by  $\gamma$ -serpentine (light) along tremolite cleavage planes. Slightly crossed polars. Scale in mm (as in b to h). (b) Sample 71-265, southern Sultan Complex. Tremolite-bastites after large elongate tremolite euhedra in a matrix of antigorite. The dominant mode of replacement is  $\gamma$ -serpentine parallel to tremolite cleavage. The relict (001) tremolite parting is preserved in several bastites, but cross-veins are not well developed. Crossed polars. (c) Sample 22N-10. Tremolite-bastite in a matrix of mesh-textured lizardite and sparse relict olivine (very bright areas). Gamma-serpentine (including extremely fine-grained opaque material) dominates over small, bipartite cross-veins that are free of magnetite. Figure 5e shows a detail of small, secondary diopside grains intergrown with this bastite. Crossed polars. (d) Sample 8-2. Feather River. Completely serpentinized tremolite composed predominantly of  $\gamma$ -serpentine with varying amounts fine-grained disseminated magnetite. Prominently developed are several cross-veins of  $\alpha$ -serpentine containing a thin central parting of magnetite. Bastite is also rimmed by  $\gamma$ -ser-

TABLE 1. MICROPROBE ANALYSES OF SECONDARY DIOPSIDE

MINERAL	1	2	3	4	5	6	7
	cpx	cpx	cpx	cpx	Trem.	Serp.	cpx
SAMPLE	71-103	71-103	71-268	71-267	71-267	71-267	---
SiO	55.4	55.3	54.9	54.7	57.6	43.7	
TiO <sub>2</sub>	0.00	0.00	0.00	n.d.	0.02	n.d.	0.07-0.28
Al <sub>2</sub> O <sub>3</sub>	0.01	0.00	0.07	0.00	0.18	0.10	1.3-4.6
Cr <sub>2</sub> O <sub>3</sub>	0.08	0.06	0.09	n.d.	0.00	0.00	0.19-0.82
MgO*	18.2	18.3	18.3	18.1	23.6	41.0	
FaO*	0.71	1.3	1.0	0.81	1.3	1.6	2.2-4.2
CaO	25.4	25.5	25.6	25.2	12.8	n.d.	
MnO	0.18	0.15	0.21	n.d.	0.07	0.14	0.10-0.16
Na <sub>2</sub> O	0.02	0.00	0.02	0.08	0.00	n.d.	0.11-0.29
NiO	n.d.	n.d.	n.d.	n.d.	0.01	0.01	
Total	100.0	100.6	100.4	99.0	95.6	86.6	
Si	2.001	1.993	1.983	1.997	8.000	4.058	
Ti	-	-	0.007	0.007	0.002	-	
Al	0.001	-	0.003	0.004	0.029	0.011	
Cr	0.002	0.002	0.003	-	-	-	
Mg	0.982	0.982	0.984	0.985	4.886	5.735	
Fe	0.022	0.040	0.031	0.025	0.151	0.121	
Ca	0.984	0.986	0.989	0.986	1.905	-	
Mn	0.005	0.005	0.007	0.008	0.008	0.011	
Na	0.001	-	0.001	0.005	-	-	
Ni	-	-	-	-	0.001	0.002	
Total	3.998	4.030	4.008	4.003	14.983	9.937	
Fe	1.1	1.4	1.5	1.2			
Wo	49.5	48.8	49.4	49.4			
En	49.4	49.8	49.1	49.4			

\*[Total Fe as FeO  
 \*Ranges of various oxides in primary clinopyroxene in Sultan Complex cumulates (Jung, 1974).  
 0.00 - indicates a concentration below the detection limit of the microprobe (0.01 percent).  
 n.d. - indicates that the element was not analyzed.  
 Column 1-4 - cations calculated on the basis of 6.0 oxygens.  
 Column 5 - cations calculated on the basis of 23.0 oxygens.  
 Column 6 - cations calculated on the basis of 14.0 oxygens.

*Secondary diopside associated with the formation of tremolite-bastites*

Where the secondary diopside occurs as relatively large grains, it is characterized by a distinctive rhombic habit. It is distinguished from rhomb-shaped tremolite euhedra by its higher relief, a tendency to assume a more irregular outline than tremolite and a lack of cleavage. Extremely fine-grained needles or aggregates of equant diopside are present in some tremolite-bastites in the absence of the more easily identified large grains. In the latter case, identification by petrographic methods is tentative, as the grains are too fine and too intimately intergrown to permit measurement of optical properties (Figs. 4g, 4h, 5i).

Sample 71-267 is a contact-metamorphosed

ultramafic rock from the southern Sultan Complex that contains narrow bands of coarse-grained tremolite up to 0.8 cm in a matrix of fine-grained serpentine (antigorite?) and magnetite. The tremolite grains are partly serpentinized and include randomly oriented diopside rhombs. Somewhat irregular, elongate patches of an isotropic phase with high relief, presumably hydrogrossular, are also present. Microprobe analyses of the tremolite, diopside and tremolite-bastite are listed in Table 1.

Sample 22N-10 (Figs. 4c, 5e, f) is an olivine-tremolite-chlorite rock from the Feather River peridotite. It contains completely serpentinized tremolite in a matrix of olivine and mesh-textured lizardite (30:70). The tremolite-bastites contain small clusters of radiating diopside rhombs. The diopside has nucleated on the margins of the bastite and on included magnetite grains and has grown at high angles to the  $\gamma$ -serpentine that formed parallel to the tremolite cleavage. The scattered clusters of secondary diopside comprise about 5% of the tremolite-bastites in which they occur.

*Secondary diopside associated with cpx-bastites*

Sample 71-268 is a serpentinite from the southern Sultan Complex that consists of approximately 50% cpx-bastites in a matrix of partly recrystallized mesh-textured lizardite, carbonate and secondary diopside (Figs. 5b, c). The diopside occurs most abundantly as clusters of rhombs radiating outward from the margins of the cpx-bastites. Fibrous mattes of much finer grained diopside crystals are intimately intergrown with the rhombs. Discrete clusters of diopside rhombs and associated needles are also present in the matrix serpentine and as aggregates surrounding altered chromian spinel grains.

The secondary diopside in sample 71-103 (also from the southern Sultan Complex) is similar to that in 71-268 in that it is relatively coarse-grained, abundant and forms rims around

pentine oriented normal to bastite margin; this appears very dark in photo. Matrix consists of mesh-textured lizardite and minor relict olivine. Crossed polars. Same scale as 4(f). (e) Sample 8-2. Unusual incipient tremolite-bastite adjacent to the one shown in 5(d). Rectangular islands of tremolite (T) are cut by two types of cross-veins. Dark, offset veins of  $\alpha$ -serpentine extend into matrix serpentine. More abundant bipartite cross-veins of  $\gamma$ -serpentine cut across tremolite with minimal offset. Early and extensive vein formation is atypical. Juxtaposition of partly and completely serpentinized tremolite (e, d) demonstrates local variations in stages of development of tremolite-bastites. Crossed polars. Same scale as 4(f). (f) Sample 8-2. Two tremolite-bastites containing variable amounts of relict tremolite. The bastite on the left has a well-developed rim of radiating  $\gamma$ -serpentine with the fibre direction oriented roughly normal to the bastite margin. Partially crossed polars. (g, h) Sample 3-1, Feather River peridotite. Two photomicrographs of the same view. Plane-polarized light on the left, partly crossed polars on the right. An aggregate of stubby tremolite grains (T) in a matrix of olivine has been partly serpentinized whereas the olivine has not. The (001) tremolite parting is poorly developed and serpentine cross-veins are absent. Dark, fine-grained aggregates of secondary diopside(?) are associated with the tremolite-bastites.

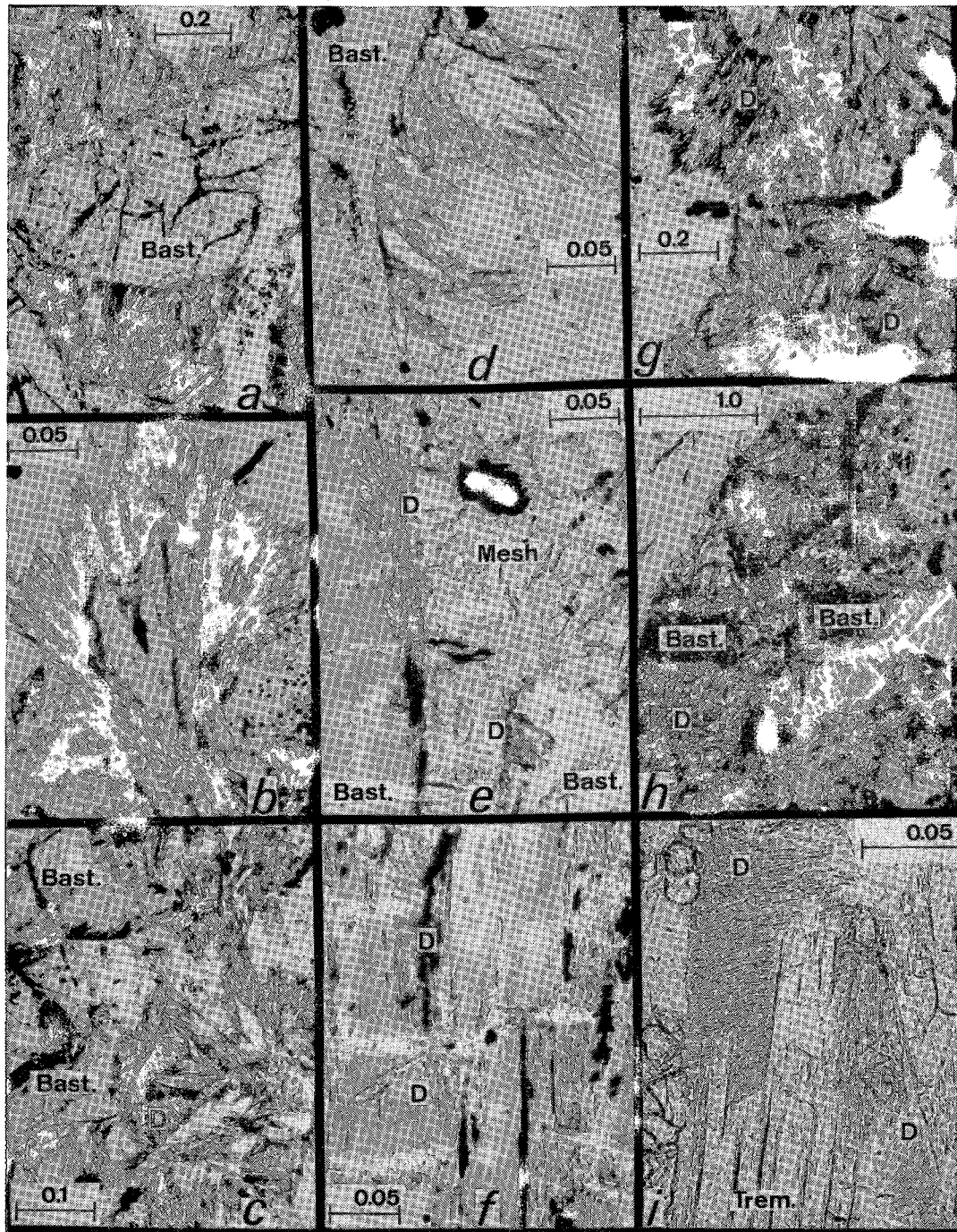


FIG. 5. Photomicrographs of secondary diopside associated with tremolite-bastites and cpx-bastites. (a) Sample 71-268. Rhomboidal diopside and associated fine-grained needles form a rim around a cpx-bastite. Note that the diopside has nucleated on the margin of the bastite and is absent from the volume of the parent pyroxene. Plane-polarized light. Scale in mm (as in b to i). (b) 71-268. Detail of a rhomb-needle combination intergrowth. This diopside has grown in matrix serpentine and has nucleated on magnetite rather than the margin of a cpx-bastite. Diameter of the needles 10-20  $\mu\text{m}$ . (c) 71-268. Rhomb-and-needle diopside partly rimming two cpx-bastites. Bastite at top is partly replaced by carbonate. Partly crossed polars. (d) High magnification of the lower left area shown in 5(e). Note similarity to secondary diopside in Figure 3. (e) Sample 22N-10, Feather River peridotite. Small, fine-grained aggregates of secondary diopside (D), which have nucleated on the margin of a tremolite-bastite. Plane-polarized light. (f) Sample 22N-10. Detail of the interior of another tremolite-bastite in which scat-

cpx-bastites and altered chrome spinel (Figs. 5g, h). There is a very strong correlation between the distribution of secondary diopside and the availability of nucleation sites provided by opaque phases. Sample 71-279 is a serpentinized websterite (Fig. 2c). A few of the cpx-bastites are partly rimmed by diopside overgrowths resembling those illustrated in Figure 3.

Table 1 lists microprobe analyses of secondary diopsides associated with cpx-bastites in 71-103 and 71-268. They are very similar to the analysis of diopside from 71-267, which formed as a result of the serpentinization of tremolite. Column 7, Table 1 summarizes the ranges of  $\text{TiO}_2$ ,  $\text{Al}_2\text{O}_3$ ,  $\text{Cr}_2\text{O}_3$ ,  $\text{FeO}$ ,  $\text{MnO}$  and  $\text{Na}_2\text{O}$  in primary clinopyroxenes from the Sultan Complex cumulates (analyses taken from Dungan 1974). A comparison of these values with analyses of secondary diopside indicates a substantial reduction in the amount of all the components except Mn. Microprobe analyses of diopside in serpentinites and metaserpentinites from other localities by Peters (1968), Trommsdorff & Evans (1972), Frost (1973) and Ehrenberg (1975) are virtually identical to those in Table 1. Taken as a whole, these data establish that secondary diopside in serpentinites has a restricted compositional range that tends to approach pure  $\text{CaMgSi}_2\text{O}_6$ .

#### *Crystallographic correspondence between the bastite-type pseudomorphs and parent silicates*

The textural relationship between bastitic lizardite and its parent silicates is very consistent and far less complex than in mesh serpentine; *i.e.*, the bastites are predominantly comprised of lizardite platelets that generally exhibit rigid parallelism to the prismatic cleavage of the parent silicates. The significance of this orientation was demonstrated by the X-ray microbeam studies of Wicks (1969), who showed that there was a three-dimensional crystallographic correspondence between intergrown lizardite and orthopyroxene. The underlying structural cause for this topotactic relationship is found in the parallelism of  $a_{\text{opx}}$  and  $c_{\text{liz}}$ , which translates into parallelism of the oxygen-anion

frameworks of the two phases. That is, the close-packed oxygens retain some structural integrity during the conversion to lizardite, whereas the cations are free to migrate (Brindley 1963). Pseudomorphism of orthopyroxene by oriented lizardite such  $a_{\text{liz}} // c_{\text{opx}}$ ,  $b_{\text{liz}} // b_{\text{opx}}$  and  $c_{\text{liz}} // a_{\text{opx}}$  also yields the following correspondence between unit-cell parameters:  $c_{\text{opx}} \simeq a_{\text{liz}}$ ,  $b_{\text{opx}} \simeq b_{\text{liz}}$  and  $3a_{\text{opx}} \simeq 4c_{\text{liz}}$  (Wicks 1969). Wicks did not determine crystallographic interrelationships between lizardite and tremolite or lizardite and clinopyroxene. However, the textural similarities among the three bastite types suggest that similar parent-bastite relations obtain.

A well-documented example of an oriented transformation between a pseudomorphous sheet silicate and a chain silicate has been described by Eggleton (1975). Here nontronite has replaced hedenbergite topotactically and with such a high degree of orientation that single crystals of nontronite result. Eggleton concluded that the ability of nontronite to form such perfect pseudomorphs is due to the oriented transformation of 1.5 unit cells of pyroxene to one unit cell of nontronite with no volume change. The nontronite exhibits the same crystallographic relationship to hedenbergite as lizardite does to orthopyroxene: ( $b_{\text{nont}} // b_{\text{hed}}$ ,  $a_{\text{nont}} // c_{\text{hed}}$  and  $c_{\text{nont}} // a_{\text{hed}}$ ).

#### PHASE RELATIONS

Recent experimental and petrological studies of progressively metamorphosed serpentinites have produced new information concerning the phase relations among amphiboles, clinopyroxene, olivine and antigorite in these rocks (Evans & Trommsdorff 1970, 1974, Trommsdorff & Evans 1972, 1974, Springer 1974, Frost 1975). One important result of this work is the recognition that there is a lack of correspondence between the serpentine mineralogy of the dehydration reactions recorded in thermally upgraded rocks and retrogressive pseudomorph-forming reactions (Evans *et al.* 1976, Dungan 1977). The critical difference is that antigorite participates in the dehydration reactions and lizardite plus minor chrysotile are the constituent phases of

---

tered, fine-grained diopside is abundant. Many small grains are oriented parallel to  $\gamma$ -serpentine. Two prominent clusters of radiating diopside (D) needles have nucleated on a magnetite segregation. Diameter of the needles is 5–10  $\mu\text{m}$ . Plane-polarized light. (g) Sample 71-103, southern Sultan Complex. Coarse-grained clusters of rhomb-shaped diopside nucleated on magnetite grains. (h) Sample 71-103. Cpx-bastites (Bast.) surrounded by secondary diopside (D). Note the concentration of diopside around the bastites. Diopside is absent from sheared serpentine in upper left of photomicrograph except at its margins. Slightly crossed polars. (i) Sample 3-1, Feather River peridotite. Fine-grained diopside (D) associated with the serpentinization of tremolite (Trem.). Micron-diameter needles have nucleated on the margin of the bastite and grown inward at high angles to the  $\gamma$ -serpentine, which has replaced the tremolite parallel to its cleavage. This photomicrograph is a detail of Figure 4 (g) and (h). Plane-polarized light.

pseudomorphs (Wicks 1969, Wicks & Zussman 1975). Until recently (Johannes 1975), chrysotile was the only serpentine phase to have been reported in experimental reversals of serpentine-olivine equilibria (Johannes 1968, Chernosky 1973). This dichotomy led Trommsdorff & Evans (1972) to postulate that natural and synthetic chrysotile-dehydration reactions were metastable relative to analogous antigorite-dehydration reactions. Evans *et al.* (1976) presented an expanded treatment of this hypothesis based in part on the recognition that chrysotile  $\rightleftharpoons$  antigorite + brucite is a reversible, naturally occurring reaction that defines the upper stability limit of chrysotile. Although lizardite-antigorite and lizardite-chrysotile phase relations are not as well documented as those between chrysotile and antigorite, many reactions in which lizardite participates may be metastable, by analogy with reactions in which chrysotile is the serpentine phase (Dungan 1977). Caruso & Chernosky (1979) argue that aluminous lizardite may have a real field of stability overlapping that of low-Al antigorite. This problem is dealt with in the companion paper (Dungan 1979).

Retrograde reactions associated with the formation of the three types of bastite pseudomorphs discussed in this paper are characterized by contradictions with equilibrium considerations based on the following observations: (1) diopside and antigorite ( $\pm$  brucite) form the stable assemblage in greenschist-facies metaserpentinities; (2) the reaction  $diop + antig \rightleftharpoons fo + trem + H_2O$  defines the upper stability-limit of diopside + antigorite; (3) orthopyroxene and serpentine have mutually exclusive stability fields and cannot be related by reversible equilibria; *i.e.*, the first appearance of enstatite in prograde reaction-sequences occurs at temperatures above the upper stability-limit of antigorite. The occurrence of secondary diopside as a reaction product of the serpentinization of clinopyroxene and tremolite and the textural relationships between this diopside and the bastite pseudomorphs provide additional confirmation of a low-temperature stability field in serpentinites.

The presence of diopside in association with tremolite-bastite suggests that the replacement occurs *via* the reaction  $fo + trem + H_2O \rightleftharpoons diop + liz$ . This reaction is the metastable analogue of the antigorite-dehydration equilibrium given above. Dungan (1977) argued that  $fo + H_2O \rightleftharpoons liz + bruc$  is similarly metastable relative to  $fo + H_2O \rightleftharpoons antig + bruc$ . Serpentinization of clinopyroxene in the Sultan Complex is inferred to occur in part because the high-temperature clinopyroxene of the cumulus wehrlites is unstable at low temperatures. The equilibration

to a stable composition seems to lead to complete pseudomorphous replacement by lizardite with or without the concomitant growth of rims of secondary diopside. The data of Caruso & Chernosky (1979) on aluminous systems demonstrate that lizardite compositions must be considered in any interpretation of serpentine parageneses. Dungan (1979) demonstrates that many pyroxene bastites are Al-rich. Tremolites in metaserpentinities are low in Al, suggesting that tremolite-bastites are Al-poor lizardites.

#### THE REACTION MODEL

Brindley & Zussman (1957) and Brindley (1963) demonstrated that lizardite-olivine intergrowths exhibit a tendency to be oriented mutually by a three-dimensional crystallographic relationship. One interpretation of the consequences of this topotactic relationship is that the replacement of one mineral by the other takes place by a mechanism of heterogeneous reaction in which the oxygen-anion framework of the parent phase is preserved and cations are free to migrate within the structure (Brindley 1963). Although serpentine pseudomorphs after olivine are complex intergrowths, data presented by Dungan (1977) suggest that the relative ease of nucleation of one phase on the other is an important factor in determining the textures and mineralogy of experimental and natural cases of serpentine-olivine reaction.

Textural relations in bastites and the X-ray data of Wicks (1969) indicate that the orientation of lizardite is more strongly controlled with respect to the parent phase in bastite than in mesh textures after olivine. Eggleton's (1975) characterization of a strongly oriented transformation of hedenbergite to nontronite emphasizes the facility with which a topotactically oriented sheet silicate can replace a chain silicate if the unit-cell dimensions of the two phases are closely comparable.

I propose that bastites form in much the same way as the nontronite-hedenbergite intergrowths discussed by Eggleton (1975). I also suggest that it is the enhanced ease of nucleation of the lizardite that follows from its inheritance of the structure of the pyroxene or amphibole that is responsible for the excursions from other modes of replacement.

Implicit in the application of the proposed mechanism of reaction to bastites is the preservation (roughly) of constant volume during the substantial gains and losses of various components during the pseudomorphic serpentinization of pyroxenes and amphiboles. The reaction model involves two related processes, nucleation and growth. Compared to the role of

nucleation, the mass balance of the growth process may be of secondary importance in determining the nature of mutual intergrowths between bastites and parent silicates. Constant-volume replacement requires a loss or gain of certain components on the scale of the pseudomorph during serpentinization. The Si excess that results from the replacement of orthopyroxene by serpentine may react with brucite (previously or simultaneously produced by the serpentinization of associated olivine grains) to produce a net gain of serpentine within the adjacent mesh pseudomorphs. Overall volume increase is reduced by the conversion of brucite to serpentine. However, the effectiveness of local chemical compensation depends on parent-silicate volume relations that rarely will be optimal. If the hydration of enstatite were otherwise isochemical, serpentine alone could not be the replacement product. The higher Si/Mg in enstatite indicates that it would be replaced by talc + serpentine at low metamorphic grade. The absence of microscopic crystals of talc intergrown with lizardite in opx-bastites indicates that Si in excess of the amount needed to form serpentine is expelled from the volume of the parent enstatite. The serpentinization of clinopyroxene involves a large loss of Ca from the volume of the parent silicate and generally does not occur until associated olivine and orthopyroxene are completely replaced. Where abundant secondary diopside is associated with cpx-bastites, it has replaced pre-existing matrix serpentine (usually mesh). This demonstrates that Ca and Si expelled from the parent clinopyroxene are balanced locally by a reverse migration of Mg into the volume of the cpx-bastite, with little volume change. The more common case, in which Ca is removed entirely from the area in which the clinopyroxene is replaced, requires corresponding migrations of Si and Mg. The occurrence of secondary diopside entirely outside the volume of the parent clinopyroxene is a significant point in support of the topotactic model. If nucleation effects were not predominant, a structureless aggregate of diopside and lizardite might result. The favored interpretation of this phenomenon is that in the initial stages of reordering of the unstable primary clinopyroxene, lizardite nucleation and growth predominate to the extent that expulsion of Ca from the structure is complete. This effect is similar to the loss of Si during formation of opx-bastites and also applies in tremolite-bastites where secondary diopside is absent or far less abundant than would be expected from the amount of Ca that must have been released.

## CONCLUSIONS

In summary, the three bastite-forming reactions occur for three different reasons. Cpx-bastites result from re-equilibration of clinopyroxene to a stable low-temperature composition. Enstatite is replaced at temperatures well below its stability field, so that the reaction is nonreversible. Tremolite-bastites are formed metastably as part of a multiphase retrograde assemblage by a reaction for which there is a prograde analogue. Despite these differences and the mass transport required to produce nearly monomineralic pseudomorphs by replacement of these three compositionally distinct parent phases, the products of low-temperature alteration of these minerals are lizardite-bastites that exhibit a remarkable degree of textural similarity. The petrographically observed parallelism and the consistency of orientation of the lizardite platelets with respect to structural elements of the parent phases, as shown by the X-ray data of Wicks (1969), imply that the reactions are topotactic. Where reactions proceed as oriented transformations, nucleation and growth of newly formed phases are greatly enhanced because of the less drastic reorganization of the parent structure inherent in this type of intergrowth. An important factor in the formation of bastites seems to be the ability of lizardite to form oriented intergrowths with orthopyroxene, clinopyroxene and tremolite. Where the parent minerals are aluminous, lizardite stability may be real and compositional control may contribute or even predominate (Caruso & Chernosky 1979).

## ACKNOWLEDGEMENTS

This research was initiated at the University of Washington, Seattle, and was partly supported by funds from NSF grant 11-2589. An early version of the manuscript was reviewed by Bernard Evans, Ron Frost, Bob Coleman and Judith Moody. The revised manuscript has also benefited by comments from Fred Wicks and Joe Chernosky. Linda Dungan, Elinor Stockon, Etta Dorman and Nazlee Coburn participated in preparation of the manuscript at various stages of its painful evolution.

## REFERENCES

- BRINDLEY, G.W. (1963): Crystallographic aspects of some decomposition and recrystallization reactions. *In Progress in Ceramic Science* (J.E. Burke, ed.), Macmillan, New York.
- & ZUSSMAN, J. (1957): A structural study of the thermal transformation of serpentine minerals to forsterite. *Amer. Mineral.* 42, 461-474.
- CARUSO, L.J. & CHERNOSKY, J.V., JR. (1979): The stability of lizardite. *Can. Mineral.* 17, 757-769.

- CHERNOSKY, J.V., JR. (1973): The stability of chrysotile,  $Mg_3Si_2O_5(OH)_4$ , and the free energy of formation of talc,  $Mg_3Si_4O_{10}(OH)_2$ . *Geol. Soc. Amer. Program Abstr.* 5, 575.
- COATS, C.J.A. (1968): Serpentine minerals from Manitoba. *Can. Mineral.* 9, 322-347.
- COLEMAN, R.G. (1971): Petrologic and geophysical nature of serpentinites. *Geol. Soc. Amer. Bull.* 82, 897-918.
- DUNGAN, M.A. (1974): *The Origin, Emplacement, and Metamorphism of the Sultan Mafic-Ultramafic Complex, North Cascades, Snohomish Country, Washington*. Ph.D. thesis, Univ. Washington, Seattle, WA.
- (1977): Metastability in serpentine-olivine equilibria. *Amer. Mineral.* 62, 1018-1029.
- (1979): A microprobe study of antigorite and some serpentine pseudomorphs. *Can. Mineral.* 17, 771-784.
- EGGLETON, R.A. (1975): Nontronite topotaxial after hedenbergite. *Amer. Mineral.* 60, 1063-1068.
- EHRENBERG, S.N. (1975): Feather River ultramafic body, northern Sierra Nevada, California. *Geol. Soc. Amer. Bull.* 86, 1235-1243.
- EVANS, B.W., JOHANNES, W., OTERDOOM, H. & TROMMSDORFF, V. (1976): Stability of chrysotile and antigorite in the serpentine multisystem. *Schweiz. Mineral. Petrog. Mitt.* 56, 79-93.
- & TROMMSDORFF, V. (1970): Regional metamorphism of ultramafic rocks in the central Alps: paragenesis in the system  $CaO-MgO-SiO_2-H_2O$ . *Schweiz. Mineral. Petrog. Mitt.* 50, 481-492.
- & ——— (1974): Stability of enstatite + talc, and  $CO_2$ -metasomatism of metaperidotite, Val d'Efra, Lepontine Alps. *Amer. J. Sci.* 274, 274-296.
- FRANCIS, G.H. (1956): The serpentine mass in Glen Urquhart, Inverness-Shire, Scotland. *Amer. J. Sci.* 254, 201-226.
- FROST, B.R. (1973): *Contact Metamorphism of the Ingalls Ultramafic Complex at Paddy-Go-Easy Pass, Central Cascades, Washington*. Ph.D. thesis, Univ. Washington, Seattle, WA.
- (1975): Contact metamorphism of serpentine, chlorite blackwall and rodingite at Paddy-Go-Easy Pass, Central Cascades, Washington. *J. Petrology* 16, 272-313.
- GARY, M., MCAFEE, R., JR. & WOLF, C.L., eds. (1972): *Glossary of Geology*, Amer. Geol. Inst., Washington, D.C.
- HADINGER, W. (1845): *Naturwissenschaftliche Abhandlungen*. Vols. 1-4, Wien.
- HEATH, M. (1971): *Bedrock Geology of the Monte Cristo Area, Northern Cascades, Washington*. Ph.D. thesis, Univ. Washington, Seattle, WA.
- HIETANEN, A. (1951): Metamorphic and igneous rocks of the Merrimac area, Plumas National Forest, California. *Geol. Soc. Amer. Bull.* 62, 565-608.
- (1973): Geology of the Pulga and Bucks Lake quadrangles, Butte and Plumas Counties, California. *U. S. Geol. Surv. Prof. Pap.* 731.
- HOCHSTETTER, R. (1965): *Zur Kenntnis der Serpentinminerale*. Ph.D. thesis, Univ. Saarlandes, Saarbrücken, Germany.
- JOHANNES, W. (1968): Experimental investigation of the reaction forsterite +  $H_2O \rightleftharpoons$  serpentine + brucite. *Contr. Mineral. Petrology* 19, 309-315.
- (1975): Zur Synthese und thermischen Stabilität von Antigorit. *Fortschr. Mineral.* 53, 1-36.
- JOHNSON, M., DUNGAN, M.A. & VANCE, J.A. (1977): Stable isotope compositions of olivine and dolomite in peridotites formed by deserpentinization, Darrington area, North Cascades, Washington. *Geochim. Cosmochim. Acta* 41, 431-435.
- KLINKHAMMER, B.F. (1962): *Ultrabasite des Ostbayerischen Grenzgebirges*. Ph.D. thesis, Univ. Saarlandes, Saarbrücken, Germany.
- PETERS, T. (1968): Distribution of Mg, Fe, Al, Ca and Na in coexisting olivine, orthopyroxene and clinopyroxene in the Totalp serpentinite (Davos, Switzerland) and in the alpine metamorphosed Malenco serpentinite (N. Italy). *Contr. Mineral. Petrology* 18, 65-75.
- SPRINGER, R.K. (1974): Contact metamorphosed ultramafic rocks in the western Sierra Nevada foothills, California. *J. Petrology* 15, 160-195.
- TROMMSDORFF, V. & EVANS, B.W. (1972): Progressive metamorphism of antigorite schist in the Bergell tonalite aureole (Italy). *Amer. J. Sci.* 272, 423-437.
- & ——— (1974): Alpine metamorphism of peridotitic rocks. *Schweiz. Mineral. Petrog. Mitt.* 54, 333-352.
- VANCE, J.A. (1972): Mid-Tertiary tectonic emplacement of metamorphic peridotites on the Darrington area, Cascade Mountains, Washington. *Geol. Soc. Amer. Program Abstr.* 4, 253.
- & DUNGAN, M.A. (1977): Formation of peridotites by deserpentinization in the Darrington area, Cascade Mountains, Washington. *Geol. Soc. Amer. Bull.* 88, 1497-1508.
- , DUNGAN, M.A., BLANCHARD, D.P. & RHODES, J.M. (1980): Tectonic setting and trace element geochemistry of Mesozoic ophiolitic rocks in western Washington. *Amer. J. Sci.* 280A, 359-388.
- WICKS, F.J. (1969): *X-ray and Optical Studies on Serpentine Minerals*. D. Phil. thesis, Oxford Univ., Oxford, England.
- & PLANT, A.G. (1979): Electron-microprobe and X-ray-microbeam studies of serpentine textures. *Can. Mineral.* 17, 785-830.
- & WHITTAKER, E.J.W. (1975): A reappraisal of the structures of serpentine minerals. *Can. Mineral.* 13, 227-243.
- & ——— (1977): Serpentine textures and serpentinization. *Can. Mineral.* 15, 459-488.
- & ZUSSMAN, J. (1975): Microbeam x-ray diffraction patterns of the serpentine minerals. *Can. Mineral.* 13, 244-258.
- WINCHELL, A.N. & WINCHELL, M. (1951): *Elements of Optical Mineralogy II*. John Wiley & Sons, New York.